

# Optical tomography with the equation of radiative transfer

A.D. Klose, A. Bluestone, M. Löcker, G. Abdoulaev, and A.H. Hielscher  
 State University of New York - Downstate Medical Center, Department of Pathology,  
 450 Clarkson Avenue, Brooklyn, New York 11203, USA  
 aklose@netmail.hscbklyn.edu

J. Beuthan  
 Laser- und Medizin-Technologie gGmbH, Institut an der Freien Universität Berlin,  
 Kraemerstrasse 6-10, 12207 Berlin, Germany  
 beuthan@zedat.fu-berlin.de

**Abstract:** We report on the implementation and experimental validation of a novel iterative image reconstruction scheme that is based on the equation of radiative transfer. Unlike schemes that are based on the diffusion equation, our scheme does not require that the transport scattering coefficient,  $\mu_s'$  is much larger than the diffusion coefficient. Furthermore, this code allows successful reconstruction of media that contain void-like regions, in which scattering and absorption coefficients are very small.

©1999 Optical Society of America

OCIS codes: (170.6960) Tomography; (170.3010) Image reconstruction techniques

## 1. Introduction:

In recent years several research groups have demonstrated limitations on diffusion theory based reconstruction schemes [1,2]. It has been shown that the diffusion equation, which is an approximation to the equation of radiative transfer, fails to describe the photon propagation in media in which the absorption coefficient is not substantially smaller than the scattering coefficient. Furthermore the diffusion equation fails in strongly heterogeneous media, which contain void-like regions in which the scattering and absorption coefficient are very small compared to the surrounding medium.

Recently Klose and Hielscher [3] have reported on an algorithm that overcomes these problems, by employing a gradient based iterative image reconstruction (GIIR) scheme that is based on the equation of radiative transfer. Similar to other GIIR schemes [4-6], the Klose-Hielscher algorithm consists of three main parts. First, an upwind differencing scheme is used that provides predicted detector readings,  $P(\zeta_k(r))$ , assuming a certain initial spatial distribution of optical properties that are expressed in an N-dimensional vector  $\zeta_{k=0}(r)$ , where N is the number of unknowns in the image. Second, an objective function,  $\Phi(\zeta_k(r))$ , which compares the measured data, M, with the predicted data,  $P(\zeta_k(r))$ , is evaluated to obtain a measure of difference between M and  $P(\zeta_k(r))$ . In a third step the initial guess  $\zeta_{k=0}(r)$  is updated by calculating  $\zeta_{k+1} = \zeta_k + \alpha A g$ , where  $g = \partial\Phi(\zeta)/\partial\zeta$  is the gradient of the objective function in column-vector form of length N, A is an NxN matrix, and  $\alpha$  is a real number. For the case of steepest gradient descent A equals the unity matrix, with only 1's on the diagonal, and  $\alpha$  is the step size in the direction of the gradient. The gradient g is calculated by the method of adjoint differentiation. The goal of the image reconstruction algorithm is to minimize the objective function  $\Phi(\zeta(r))$ . The distribution  $\zeta(r)$  that minimizes  $\Phi(\zeta(r))$  is the desired cross-sectional image.

While successful in overcoming deficiencies of diffusion-based algorithm, the Klose-Hielscher codes has its weaknesses. It is slow and as all gradient based schemes prone to find local rather than global minima of the objective function. In this work we go beyond the gradient based scheme in two major ways. First the current Jacobian-scheme for the forward model is replaced with a much more efficient successive Gauss-Seidel, successive-overrelaxation technique. Second the gradient-scheme is replaced with a Newton-type scheme that employs second derivative information,  $h = \partial^2\Phi(\zeta)/\partial\zeta_i\partial\zeta_j$  for the update. With these changes the speed of the reconstruction scheme could be improved at least by a factor of 20. Furthermore, the new forward and reconstruction schemes are numerically and experimentally tested.

## 2. Methods

### 2.1. Forward model

The fundamental quantity in radiative transport theory is the radiance  $\Psi(r, \Omega)$  at the spatial position r, which is directed into a unit solid angle  $\Omega$ . Its unit is  $W\text{ cm}^{-2}\text{ sr}^{-1}$ . The photon transport is described by the time-independent equation of radiative transfer, which is an integro-differential equation

$$\omega \cdot \nabla \Psi(r, \omega) + (\mu_a + \mu_s) \Psi(r, \omega) = S(r, \omega) + \mu_s \int_0^{2\pi} p(\omega, \omega') \Psi(r, \omega') d\omega' \quad (1)$$

To solve the equation for radiative transfer using a discrete-ordinate finite-difference method the angular and spatial variables have to be discretized. First, the integral term is replaced by a quadrature formula that uses a finite set of angular directions. This yields a set of coupled ordinary differential equations for the angular-dependent radiance  $\Psi_k(r) = \Psi(r, \omega_k)$  in the directions  $\omega_k$ . Additionally, the spatial variable  $r$  needs to be discretized. Therefore, the domain  $\Omega$  is defined by a rectangular spatial mesh with  $M$  grid points on the  $x$ -coordinate and  $N$  grid points on the  $y$ -coordinate. Finally, the spatial derivatives have to be replaced with a finite-difference scheme. In this work we use an upwind-difference scheme. The transport equation, with the external and internal source term on the right-hand-side, can be written as:

$$\mu_k \frac{\Psi_{k,i,j} - \Psi_{k,i-1,j}}{\Delta x} + \eta_k \frac{\Psi_{k,i,j} - \Psi_{k,i,j-1}}{\Delta y} + (\mu_a + \mu_s) \Psi_{k,i,j} = S_{k,i,j} + \mu_s \sum_{k'=1}^K a_{k'} p_{k,k'} \Psi_{k',i,j} \quad (2)$$

or shorter in matrix form  $\mathbf{A}\Psi = \mathbf{b}$ . The resulting system of equations for the radiance  $\Psi_{ij}$  for all grid points is solved for each ordinate index  $k$  by a *Gauss-Seidel method* [7,8]. Therefore we split the matrix  $\mathbf{A}$  into a diagonal part  $\mathbf{D}$  of  $\mathbf{A}$ , an upper part  $\mathbf{U}$  of  $\mathbf{A}$ , and a lower part  $\mathbf{L}$  of  $\mathbf{A}$  with  $\mathbf{A} = \mathbf{L} + \mathbf{D} + \mathbf{U}$ . Now the iterative form with the iteration matrix  $(\mathbf{D} + \mathbf{L})$  is expressed as:

$$(\mathbf{D} + \mathbf{L})\Psi^{n+1} = -\mathbf{U}\Psi^n + \mathbf{b} \quad (3)$$

A significant improvement in convergence speed can be achieved by a slight modification of the *Gauss-Seidel method*. The *Successive-Overrelaxation Method (SOR)* [7,8] uses a relaxation parameter  $\omega$  with  $1 < \omega < 2$  in order to correct the solution  $\bar{\Psi}_{k,i,j}^{n+1}$  of the *Gauss-Seidel iteration*. The accepted new value  $\Psi_{k,i,j}^{n+1}$  is extrapolated from the *Gauss-Seidel* value and the previous accepted value  $\Psi_{k,i,j}^n$  with  $\Psi_{k,i,j}^{n+1} = (1 - \omega)\Psi_{k,i,j}^n + \omega\bar{\Psi}_{k,i,j}^{n+1}$ . In between each iteration step  $n$  the boundary conditions are treated. Assuming partly reflective Fresnel boundary conditions the angular radiance  $\Psi_{k,i,j}^n$  can be calculated at the boundary grid points for each ordinate  $\omega_k$  for given refraction indices.

## 2.2. Updating scheme

The minimum of  $\Phi(\zeta(r))$  is typically found by employing information about the gradient  $d\Phi(\zeta(r))/d\zeta(r)$ . In the past several groups have developed steepest-gradient-descent (SGD) techniques, while our group has favored the conjugate gradient (CG) method [3,5]. These methods have shown some good results, however they are known to be only slowly converging and sensitive to local minima. To alleviate these disadvantages we have implemented in this work a full quasi-Newton (FQN) and limited-memory-quasi-Newton (LMQN) method, using a Broyden-Fletcher-Goldfarb-Shanno (BFGS) approach [7,8]. The quasi-Newton techniques, also often called variable metric methods, employ information about the second derivative  $\partial^2 \Phi(\zeta(r))/\partial \zeta(r_i) \partial \zeta(r_j)$  (Hessian) in the reconstruction process.

## 3. Results:

The accuracy of the reconstruction scheme evaluated with experimental data of a transilluminated tissue-like scattering phantom. The phantom was a composition of titanium dioxide spheres embedded in epoxy resin. The size of the phantom was  $3 \times 3 \times 14 \text{ cm}^3$ . The reduced scattering coefficient was  $\mu_s' = 11.6 \pm 0.3 \text{ cm}^{-1}$  and the absorption coefficient was  $\mu_a = 0.35 \pm 0.04 \text{ cm}^{-1}$ . The anisotropy coefficient was approximately  $g = 0.86 \pm 0.02$ . Inside the medium was a ring with a width of 3mm that did not contain any titanium dioxide (Fig. 1a). The phantom was continuously illuminated with four point sources (laser diodes at wavelength  $\lambda = 670 \text{ nm}$ ), each in the center of each side. As a detector we used an avalanche photo diode APD. The detector was placed in the  $x$ - $y$  plane and could be moved around the phantom along the  $x$ -axis and  $y$ -axis, respectively. The outgoing fluence rate was measured at 30 points along the  $x$ -axis and the  $y$ -axis except from the side of laser incident. The calculated fluence was compared to the measured data on the boundary of the phantom. We only compared relative fluence profiles on the boundary and not absolute fluence rates. This situation is typically encountered in clinical settings, because of the difficulty in calibrating the system to an accurate absolute value of the source strength. Thus, the measurement data and simulated data were normalized by their mean value and we obtained a normalized fluence profile as a function of the detector position. The data was input to the iterative reconstruction algorithm based on the equation of radiative transfer as well as a diffusion-equation-based algorithm, described in detail elsewhere.

Fig. 1b shows the result obtained with the transport code. The initial guess was  $\mu_s = 11.0 \text{ cm}^{-1}$  and  $\mu_a = 0.35 \text{ cm}^{-1}$ . The reconstructed image based clearly shows a ring with a decreased scattering coefficient of, even though the absolute value of  $\mu_s = 4.5 \text{ cm}^{-1}$  is too large. This can mainly be attributed to the initial guess, which is much larger than the actual value in the ring region. The reconstruction code based on the diffusion model (Fig. 1c) completely fails to recover the ring structure and the absolute values of scattering coefficients.

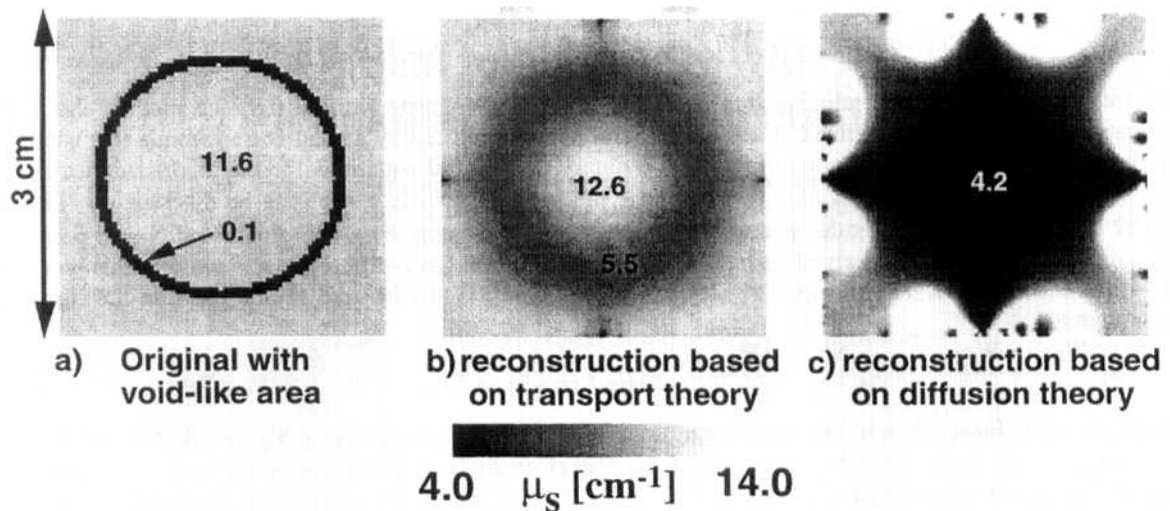


Fig. 1: a) Geometry of original tissue phantom made epoxy resin with titanium oxid particles. b) Reconstruction result from experimental data based on the equation of radiative transfer. c) reconstruction result with diffusion equation based algorithm.

Furthermore, we tested how the use of second derivative information improved the image quality and reconstruction speed. This objective function  $\Phi(\zeta(r))$  is iteratively mini-minized using the CG, FQN, or LMQN method. Figure 2 displays the value of  $\Phi$  as a function of the number of updates of the optical property distribution  $\zeta(r)$ . The results show that the quasi-Newton algorithms are superior to the conjugate-gradient technique both in terms of conversion time and image quality. Both techniques recover the position of the ring objects. However, for a fixed number of updates of the optical properties the quasi-Newton methods achieve a smaller objective function (Fig. 2) than the conjugate gradient method. The major disadvantage of quasi-Newton techniques is the large memory requirement. Our study shows that this problem can be alleviated when LMQN methods are used. For an image with  $N$  unknown pixels (here optical properties) the LMQN algorithm requires  $N$ -times less memory than the FQN algorithm, while image quality achieved with the LMQN technique is only slightly worse than the one obtained with the FQN method (Fig 1c, 1d and 2).\*

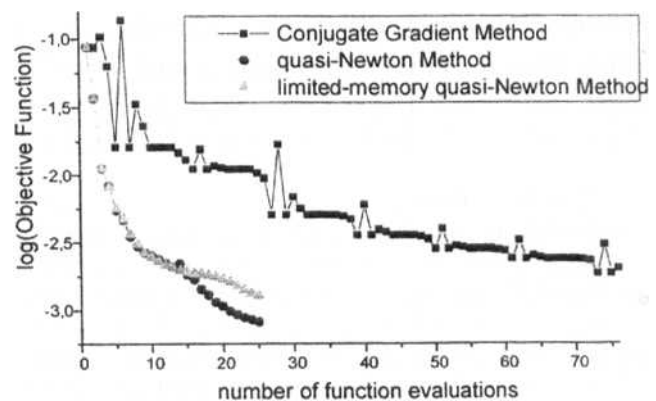


Fig. 2: Logarithm of the objective function  $\Phi(\zeta(r))$  as a function of number of updates of the optical property distribution  $\zeta(r)$ . The updates are obtained with the conjugate gradient, full quasi-Newton, and limited-memory quasi-Newton method.

#### 4. References

- [1] M. Firbank, S. R. Arridge, M. Schweiger, and D. T. Delpy, "An investigation of light transport through scattering bodies with non-scattering regions," *Phys. Med. and Biol.* **41**, 767-783 (1996).
- [2] A. H. Hielscher, R. E. Alcouffe, and R. L. Barbour, "Comparison of finite-difference transport and diffusion calculations for photon migration in homogeneous and heterogeneous tissues," *Physics in Medicine and Biology* **43**, 1285-1302 (1998).
- [3] A.D. Klose and A.H. Hielscher, "Iterative reconstruction scheme for optical tomography based on the equation of radiative transfer," *Medical Physics* **26**, 1698-1707 (1999).
- [4] S. R. Arridge and M. Schweiger, "A gradient-based optimisation scheme for optical tomography," *Optics Express* **2** (6), 213-226 (1998).
- [5] A.H. Hielscher, A.D. Klose, K.M. Hanson, "Gradient-based iterative image reconstruction scheme for time-resolved optical tomography," *IEEE Tran.s. Med. Imag.* **18**, 262-271 (1999).
- [6] R. Roy and E.M. Sevick-Muraca, "Truncated Newton's optimization scheme for absorption and fluorescence optical tomography: Part 1 Theory and formulation," *Optics Express* **10**, 353-371 (1999).
- [7] W. F. Ames, "Numerical Methods for Partial Differential Equations," (Academic Press, New York, 1977)
- [8] W. H. Press, S. A. Teukolsky, W. T. Vetterling, and B. P. Flannery, *Numerical Recipes in C* (Cambridge Univ.Press, New York, 1992).

\* This work was supported in part by The Whitaker Foundation (grant # 98-0244), the City of New York Council Speaker's Fund for Biomedical Research: Toward the Science of Patient Care., and the National Institute of Arthritis and Musculoskeletal and Skin Diseases, a part of the National Institute of Health (grant # R01 AR46255-01)